

Costs of dust collection by *Trichodesmium*: effect on buoyancy and toxic metal release

Siyuan Wang^{1,2}, Futing Zhang^{1,2}, Coco Koedooder^{1,2,3}, Odeta Qafoku⁴, Subhajit Basu^{1,2,5}, Stephan Krisch⁸, Anna-Neva Visser^{1,2}, Meri Eichner⁶, Nivi Kessler^{1,2,9}, Rene M. Boiteau⁷, Martha Gledhill⁸ and Yeala Shaked^{1,2}

¹ The Freddy and Nadine Herrmann Institute of Earth Sciences, Edmond J. Safra Campus, Givat Ram, Hebrew University of Jerusalem, Jerusalem, Israel

² The Interuniversity Institute for Marine Sciences in Eilat, Eilat, Israel

³ Israel Limnology and Oceanography Research, Haifa, Israel

⁴ Environmental Molecular Sciences Laboratory (EMSL), Pacific Northwest National Laboratory (PNNL), Richland, WA, 99454, USA

⁵ University of Petroleum and Energy Studies (UPES-SoHST), Energy Acres, Dehradun 248007, India

⁶ Center Algatech, Institute of Microbiology of the Czech Academy of Sciences, Novohradská 237, 37981 Třeboň, Czech Republic

⁷ Department of Chemistry, University of Minnesota, Minneapolis, MN 55455

⁸ GEOMAR, Helmholtz Center for Ocean Research, Kiel, Germany

⁹ Present address: The water authority, 7 Bank of Israel st, Jerusalem 9195021, Israel

Corresponding author: Yeala Shaked

Email: yeala.shaked@mail.huji.ac.il

29 The marine cyanobacterium *Trichodesmium* has a remarkable ability to interact with and utilize air-
30 borne dust as a nutrient source. However, dust may adversely affect *Trichodesmium* through
31 buoyancy loss and exposure to toxic metals. Our study explored the effect of desert dust on
32 buoyancy and mortality of natural Red Sea puff-shaped *Trichodesmium thiebautii*. Sinking velocities
33 and ability of individual colonies to stay afloat with increasing dust loads were studied in
34 sedimentation chambers. Low dust loads of up to ~400 ng per colony did not impact initial sinking
35 velocity and colonies remained afloat in the chamber. Above this threshold, sinking velocity
36 increased linearly with the colony dust load at a slope matching prediction based on Stoke's law.
37 The potential toxicity of dust was assessed with regards to metal dissolution kinetics, differentiating
38 between rapidly released metals that may impact surface blooms and gradually released metals
39 that may impact dust-centering colonies. Incubations with increasing dust concentrations revealed
40 colony demise, but the observed lethal dose far exceeded dust concentrations measured in coastal
41 and open ocean systems. Removal of toxic particles as a mechanism to reduce toxicity was explored
42 using SEM-EDX imaging of colonies incubated with Cu-minerals, yet observations did not support
43 this pathway. Combining our current and former experiments, we suggest that in natural settings
44 the nutritional benefits gained by *Trichodesmium* via dust collection outweigh the risks of buoyancy
45 loss and toxicity. Our data and concepts feed into the growing recognition of the significance of
46 dust for *Trichodesmium*'s ecology and subsequently to ocean productivity.

48 Plain Language Summary

49 The abundant marine phytoplankton *Trichodesmium* spp. are nitrogen-fixing cyanobacteria that
50 form extensive blooms in low latitude warm oceans and contribute significantly to carbon (C) and
51 nitrogen (N) fixation, recycling and export. Desert dust deposited on the ocean surface is an
52 important nutrient source for *Trichodesmium*. Spherical, millimeter-sized colonies of
53 *Trichodesmium* from different ocean basins were reported to strongly interact with dust and shuffle
54 dust particles to the colony core. While dust collection can optimize nutrient supply, it may come at
55 a cost to *Trichodesmium*. Heavy dust loads may send the colonies to the deep ocean and metal
56 release from dust may induce toxicity. Here, experimenting with Red Sea colonies and desert dust
57 we studied some of the trade-offs of dust collection. Interacting colonies with dust, we examined
58 the link between dust load and colony buoyancy. Combining dust dissolution measurements and
59 mortality assays we examined toxicity thresholds for *Trichodesmium* surface blooms and dust-
60 collecting colonies. We also studied the ability of colonies to remove particles and the effect of
61 particle loss on their sinking velocity. Our experimental findings and concepts are valuable for
62 assessing *Trichodesmium*'s distribution and ecophysiology and contribute to modeling of C or N
63 transport to the deep ocean.

64

65 Key Points

- 66 ● Dust collected by *Trichodesmium* colonies from seawater as a nutrient source may result in
67 metal toxification and buoyancy loss.
- 68 ● At moderate dust loads colonies maintained their buoyancy, but above a threshold sinking
69 velocities increased linearly with dust loads.
- 70 ● Desert dust induced *Trichodesmium* mortality through toxic metal release, but the lethal dose
71 far exceeded oceanic dust concentrations.

72

73 1. Introduction

74 *Trichodesmium* spp. is a filamentous, N₂-fixing, and bloom-forming cyanobacterium inhabiting
75 subtropical and tropical oligotrophic ocean regions and contributing ~40% of the annual global
76 marine nitrogen fixation (Capone et al., 1997; Tang et al., 2020; Zehr & Capone, 2020).
77 *Trichodesmium* spp. appear both as individual filaments (trichomes) and as colonies containing
78 hundreds to thousands of trichomes organized in millimeter-sized tuft- or puff-shaped aggregates
79 (Eichner et al., 2023). In the Red Sea, puff-shaped colonies are primarily composed of
80 *Trichodesmium thiebautii* while tuft-shaped colonies are typically comprised of *Trichodesmium*
81 *erythraeum* (Koedooder et al., 2022). The different colony morphologies also serve as micro-
82 habitats for diverse microbes including bacteria, phytoplankton and even zooplankton, all
83 exchanging nutrients and carbon throughout the colony life cycle from growth to demise (Anderson,
84 1977; Frischkorn et al., 2018; Lee et al., 2017; Rouco et al., 2016).

85 Natural *Trichodesmium* is often limited or co-limited by iron (Fe) and phosphorus (P) (Cerdan-Garcia
86 et al., 2022; Held et al., 2020). Aerosol dust deposited on the ocean surface is considered an
87 important nutrient source, but the low solubility of Fe and P minerals restricts its bioavailability for
88 phytoplankton (Mills et al., 2004; Shaked et al., 2023; Shaked & Lis, 2012; Stockdale et al., 2016).
89 Incubation studies revealed that *Trichodesmium* successfully grow on aerosol or dust (Chen et al.,
90 2011; Polyviou et al., 2018) and even increase the bioavailability of dust Fe and P (Basu et al., 2019;
91 Basu & Shaked, 2018; Shaked et al., 2023). An intriguing finding, which was reaffirmed in several
92 studies is the ability of *Trichodesmium* colonies to actively collect and transport dust particles into
93 the colony core (Kessler, Armoza-Zvuloni, et al., 2020; Rubin et al., 2011; Wang et al., 2022), which
94 may serve to enhance dust dissolution, minimize nutrient loss by diffusion and optimize uptake
95 (Eichner et al., 2023; Shaked et al., 2023). While these nutritional benefits are well established, yet
96 studies exploring negative sides of particle collection to *Trichodesmium* remain scarce. Collection of
97 heavy dust minerals may result in buoyancy loss and accelerate sinking to the deep ocean (Held et
98 al., 2022; Pabortsava et al., 2017). Dust also contains an array of toxic elements (Bozlaker et al.,
99 2013; Mackey et al., 2015), which upon gradual release within the colony core may induce toxicity
100 and cause mortality. Our study focuses on this “dark side” of particle collection by, firstly,
101 investigating the effect of dust on buoyancy and trace metal exposure of *Trichodesmium* and,
102 secondly, examining active particle removal.

103 Depending on composition, dust particle density was reported to range from 2.1 to 2.6 g·cm⁻³
104 (McConnell et al., 2008; Schladitz et al., 2009), much denser than *Trichodesmium* with density of ~1
105 g·cm⁻³ (J. Kromkamp & Walsby, 1992; White et al., 2006). Consequently, collection of dust particles
106 by *Trichodesmium* colonies increases their density and may affect *Trichodesmium's* buoyancy.
107 *Trichodesmium* spp. regulates its buoyancy through gas vesicles which can withstand high pressures
108 (up to 12-37 bars, Walsby, 1992). This allows *Trichodesmium* to float on the water surface while
109 also being able to resist hydraulic forces and conduct vertical migration to several hundred or
110 thousand meters (Benavides et al., 2022; Pabortsava et al., 2017; Walsby, 1992). While a recent
111 study modeled the effect of dust on sinking velocities of *Trichodesmium* (Held et al., 2022),
112 experimental evidence linking dust loads and sinking velocities are missing.

113 Dust and other aerosols contain an array of elements, some of which are required as nutrients,
114 while others such as cadmium (Cd), copper (Cu), lead (Pb) and arsenic (As) can be toxic (Guo et al.,
115 2022; Mackey et al., 2012; Paytan et al., 2009; Yang et al., 2019). The potential toxicity of dust (or
116 other aerosols) to *Trichodesmium* depends on the kinetics of toxic metal release to seawater, which
117 in turn vary with aerosol types and sources, reactions occurring during atmospheric transport and
118 particle to solvent ratios (Mackey et al., 2015; Mahowald et al., 2018; Stockdale et al., 2016).
119 Natural populations of *Trichodesmium* colonies are reported to be very sensitive to toxic metals
120 such as Cu and As (Hewson et al., 2009; Rueter et al., 1979). In addition to metals released from
121 dust to the seawater surrounding natural *Trichodesmium*, the collection of dust within colonies
122 further exposes them to toxic metals which gradually dissolve from the particles. However, dust
123 toxicity to *Trichodesmium*, especially at the level of individual colonies, is poorly understood.

124 Our study focuses on this “dark side” of particle collection by investigating the effect of dust on
125 buoyancy and trace metal exposure of *Trichodesmium* and examining active particle removal. These
126 effects were investigated through two sets of experiments with natural *Trichodesmium* colonies: 1)
127 sedimentation experiments with single colonies artificially loaded with dust, and 2) incubations with
128 increasing dust concentrations probing mortality and metal release rates. The ability of
129 *Trichodesmium* to mitigate these effects through particle removal was also examined. This research
130 highlights potential trade-offs associated with particle collection and may contribute to predicting
131 *Trichodesmium's* vertical distribution and role in C and N export to the deep ocean.

132

2. Material and methods

2.1 Colony & dust collection

Trichodesmium colonies were collected from the Gulf of Aqaba (29.56°N, 34.95°E) at the Northern Red Sea via net tows during 2018-2022. Each tow was conducted for ~7 min at the boat's minimal speed (1-2 knots) by deploying a 100 µm phytoplankton net (Aquatic Research Instrument, USA) to 10-20 m depth. The net concentrate was diluted into ~5 L seawater to minimize stress and well-shaped puff colonies were quickly hand-picked by droppers, placed in clean Petri dishes and washed three times with 0.22 µm filtered seawater (FSW). Dust samples were collected from the Gulf of Aqaba shores at the Inter-University Institute for Marine Sciences in Eilat (IUI). Samples of settled dust were collected from plastic surfaces located ~2 m from the sea, sieved through a 63 µm mesh, air-dried and stored in a desiccator.

2.2 Effect of dust load on colony buoyancy

Sedimentation experiments – During autumn 2020, sedimentation experiments were conducted on five consecutive days, on each testing five different colonies. Sinking velocities were measured in 18 cm tall sedimentation chambers (100 mL glass cylinders with 2.5 cm diameter). Colonies were gently introduced to chambers filled with fresh seawater and their vertical positions were recorded over time (see Fig. S1 for a schematic diagram and further details). Two types of data were collected: Initial colony sinking velocities in the chamber and colony positions in the chamber after 15 min. Each colony was tested three times: as is, and following interactions with medium and then high dust concentrations. All colonies were initially sinking and hence the sinking velocities were always positive. However, after 15 min colonies appeared to adjust their buoyancy and resumed different positions in the chamber. The ones at the bottom of the sedimentation chamber were defined as “sinkers” and the ones further up in the water as “floaters”. Colony-dust interactions were induced by gently and repetitively mixing colonies within an eppendorf vial which contained seawater with the respective amount of dust. The dust load (weight) on each colony was calculated from stereoscopic images taken prior to introducing the colonies to the sedimentation chamber. Since many colonies lost dust particles during the experiments, another image was taken at the end of each experiment and dust weight was re-calculated.

Estimation of colony dust loads – Dust load (weight) was estimated from colony images taken with a stereoscope (Nikon, SMZ745). Using DinoCapture 2.0 and ImageJ software, the area of dust centered by the colony (μm^2) was estimated. This area was converted to volume (μm^3) assuming a constant thickness of 10 μm for the dust layer and then to mass using an average density of 2.5 $\text{g}\cdot\text{cm}^{-3}$ (see Fig. S2 for details; Kessler, Kraemer, et al., 2020). Similar analysis was done on published images of dust-containing colonies (Held et al., 2021).

Calculating the effect of dust on colony sinking velocities – Stoke's law and its modified equations has been widely applied in calculating and modeling sinking velocities of marine aggregates including natural *Trichodesmium* colonies (Jacco Kromkamp & Walsby, 1990; Laurenceau-Cornec et al., 2020; White et al., 2006). Recently, several attempts were made to assess the density change induced by internal ballasts (Benavides et al., 2022; Held et al., 2022). When colonies collect dust not only its mass needs to be considered but also its volume. To account for both, dust mass and volume, the Stoke's law-based equation, adapted for *Trichodesmium* by White et al. (2006), was modified (supplementary text S1). Based on this modified equation, the colony sinking velocity is predicted to increase linearly with dust load:

$$\text{Equation. 1 Sinking velocity (dust-loaded colony) (m}\cdot\text{d}^{-1}) = \\ \text{Sinking velocity (dust-free colony) (m}\cdot\text{d}^{-1}) + K (\text{m}\cdot\text{d}^{-1}\cdot\text{ng}^{-1}) \times \text{dust weight (ng)}$$

The dust factor (K) is the velocity increase per dust mass with a unit of $\text{m}\cdot\text{d}^{-1}\cdot\text{ng}^{-1}$. Applying the measured colony size and the density of dust, Red Sea seawater and *Trichodesmium* cells (Basu & Shaked, 2018; Benaltabet et al., 2022; McConnell et al., 2008; Schladitz et al., 2009; White et al., 2006), we calculated that $K=0.02\text{-}0.06 (\text{m}\cdot\text{d}^{-1}\cdot\text{ng}^{-1})$ (supplementary text S2).

2.3 Metals in dust and toxicity to *Trichodesmium*

Dust dissolution experiments – Dust dissolution experiments were conducted in four separate experiments during 2015, using trace metal clean procedures, as described in Basu et al. (2019) and Gledhill et al. (2019). Local Red Sea dust was added to acid-cleaned Nalgene bottles containing gravimetrically quantified filtered seawater at final concentrations of 2 and 10 $\text{mg}\cdot\text{L}^{-1}$ and incubated at 25°C for 62 hours. 60 mL sub-samples were filtered through 0.22 μm syringe-filters (PVDF, Millex) using a Dynamax (Rainin) 8-head peristaltic pump under a clean bench. Sub-samples were stored for 6 months in trace metal cleaned high density polyethylene (HDPE) bottles and acidified to pH

190 ~1.7 with ultra-clean HNO_3 prior to analysis of metals. Metals were analyzed by inductively coupled
191 plasma mass spectrometry after preconcentration (SeaFAST pico) following the method of Rapp et
192 al. (2017) and were quantified by standard addition (Krisch et al., 2022) at GEOMAR, Helmholtz
193 Centre for Ocean Research, Kiel, Germany. Extending our experiments we also included dissolution
194 measurements of local Red Sea dust samples from Mackey et al. (2015). We then split the
195 dissolution data to two groups: 1) rapid dissolution (10 min and 6 h), and 2) gradual dissolution (1, 3
196 and 7 days).

197 Toxicity assays – Dust toxicity was investigated by incubating ~180 individual natural
198 *Trichodesmium* colonies for 24 h in 48 well-plates with either dust suspension or dust leachate.
199 Primary dust suspension was prepared daily in FSW and diluted to final concentrations of 2, 10, 100,
200 500, and 1000 $\text{mg}\cdot\text{L}^{-1}$. Dust leachates were obtained after 10 min by filtering the dust suspensions
201 through 0.22 μm syringe-filters (PC membrane). Colonies were incubated in wells of a 48-well plate
202 containing 0.5 mL dust suspension or leachate and were kept in a culture room (25 °C, $\sim 80 \mu\text{E m}^{-2} \text{s}^{-1}$,
203 10:14 h light-dark cycle). Visual changes of the colony and filament shape, structure, and color
204 were monitored under a stereoscope at 2, 5, and 24 h (supplementary text S4). Incubations were
205 repeated twice during spring 2022 and included controls without dust additions. Probing specifically
206 for Cu toxicity, colonies were also incubated with dissolved Cu (5-3000 nM CuSO_4 , supplementary
207 text S4).

208 2.4 Removal of Cu-containing minerals

209 Hypothesizing that colonies may remove toxic minerals as a detoxification mechanism, 16 Red Sea
210 colonies were incubated with the Cu mineral malachite ($\text{Cu}_2\text{CO}_3(\text{OH})_2$). To ensure optimal colony-
211 mineral interactions, malachite was mixed with hematite ($\alpha\text{-Fe}_2\text{O}_3$), which is typically preferred by
212 *Trichodesmium*. Individual colonies were sampled at different time points, placed on filters and
213 probed for the presence of malachite via light microscopy and scanning electron microscopy with
214 energy dispersive X-Ray analysis (SEM-EDX). Experiments were repeated for three days in autumn
215 2021. Malachite was obtained from Timna National Park (Eilat, Israel), crushed and sieved ($<38\mu\text{m}$),
216 while hematite ($<38\mu\text{m}$) was obtained from the Mineral Collection at the National Natural History
217 Collections at the Hebrew University of Jerusalem. Colonies were incubated in eppendorf vials
218 under the IUI pier up to 24 hrs. At three time points, randomly selected colonies were imaged and

219 placed on a PES membrane filter (Supor®), air-dried and frozen prior to SEM-EDX analysis (see
220 supplementary text S5 for full details).

221 [Microscopic SEM-EDX imaging](#) – Colonies were placed on Supor® filters and coated with a ~10 nm
222 carbon layer by thermal evaporation using a 108C Auto Carbon Coater (Ted Pella, Inc.) to avoid
223 charging during the analysis. SEM images were collected with a FEI Helios NanoLab 600i field
224 emission electron microscope. Specimen morphology was examined using a secondary electron
225 Everhart-Thornley detector (ETD) in a field free mode at an acceleration voltage of 3 kV and a probe
226 of 86 to 170 pA at 4 mm working distance. EDX analysis was performed at 10 to 20 kV and 1 to 2 nA
227 with an X-Max 80mm² Silicon Drift Detector (SDD) from Oxford Instruments. Oxford AZtec software
228 was used to collect compositional maps and point spectrum analyses.

229

3. Results and discussion

3.1 Dust loads and buoyancy control

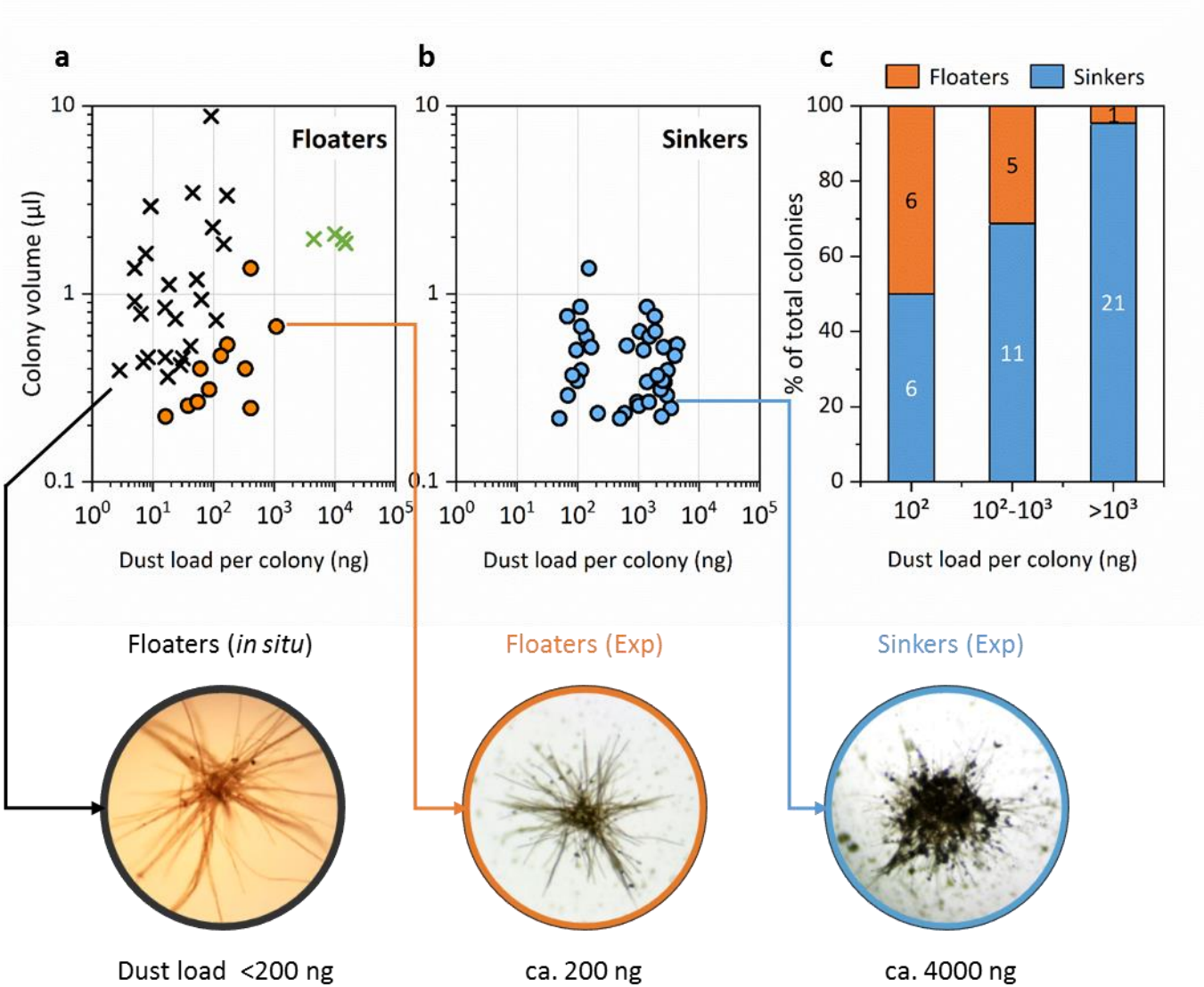
Collection and centering of dust particles by *Trichodesmium* colonies may result in buoyancy loss and enhance their sinking velocities to the ocean depth. In the following section we present experimental results of natural colonies that were interacted with dust and tested in sedimentation chambers. The impact of dust on the colony buoyancy was examined by two different measures: 1) initial, short-term (~5 min) sinking velocity, and 2) colony position in the chamber after a 15 min acclimation period. All colonies had positive initial sinking velocities, but within 15 minutes some colonies left the chamber bottom and were re-suspended in the water. Colonies that remained on the bottom were considered as non-buoyant ("sinkers"), while those in the water were considered as buoyant ("floaters").

3.1.1 How much dust can a colony bear to stay afloat?

At low dust loads (<100 ng) half of the colonies were classified as "floaters" (Fig. 1, orange symbols). At intermediate dust loads of 100-1000 ng, the fraction of "floaters" dropped but still accounted for ~30% of the colonies (Fig. 1, orange symbols). These findings demonstrate a remarkable ability of *Trichodesmium* to adjust their buoyancy to accommodate a significant dust load, assisted by their gas vesicles (Walsby, 1992). At increasing dust loads, and especially above 1 µg dust per colony, most colonies were defined as "sinkers" (Fig. 1, blue symbols), indicating a limit to *Trichodesmium's* capacity to adapt its buoyancy.

Expanding the experimental data to natural conditions, dust loads associated with Red Sea *Trichodesmium* colonies collected from the upper 10-20 meters during 2018/19 were analyzed. These colonies were considered buoyant since they populated the upper water column and were plotted together with the experimentally determined "floaters" (Fig. 1a). Each colony typically contained 1-7 particles in sizes ranging between 10-70 µm in diameter (Table S1). The calculated weight of these particles amounted to 3-170 ng per colony and did not correlate with the colony volume (Fig. 1a, black crosses). These estimated dust-loads of floating, naturally occurring colonies, matched our experimental findings (Fig. 1a, orange circles). Similar weights of 200-300 ng dust per colony were also reported by Kessler et al. (2020), who analyzed SEM images of colonies collected from the upper 20 meters of the Gulf of Aqaba (Kessler, Kraemer, et al., 2020). Interestingly, the

259 Red Sea colonies fall short compared to Atlantic colonies collected from 20 m that remain afloat
 260 with much higher particle loads (Bif & Yunes, 2017; Held et al., 2021). Analyzing single colony
 261 images from the study of Held et al. (2021), we calculated dust loads of up to 10 μg per colony (Fig.
 262 1a, green crosses). The ability to keep afloat with a higher dust load may stem from larger number
 263 of filaments in the colonies from the Atlantic compared with those from the Red Sea colonies.
 264 Based on these experiments and observations, we draw the threshold of dust that Red Sea puff-
 265 shaped colonies can bear and stay afloat at few hundred nanograms.



266

267

268 **Figure 1. Effect of dust load on the buoyancy of natural *Trichodesmium* colonies.**

269 Data compilation from natural colonies either containing particles when collected (crosses) or interacted
 270 with dust and tested in sedimentation experiments (circles). Colonies were categorized as “floaters” or
 271 “sinkers” according to their position in sedimentation chambers after 15 min. *In situ* colonies were defined
 272 as “floaters” since they were collected from the upper water column for 10-20 m depth.

- 273 (a) Range of dust loads associated with “floater” colonies tested in sedimentation experiments (n=12,
274 orange circles) and freshly collected from the Red Sea (n=24, black crosses) and the Atlantic Ocean (n=4,
275 green crosses, images from Held et al., 2021).
- 276 (b) Range of dust loads associated with “sinker” colonies tested in sedimentation experiments (n=38, blue
277 circles).
- 278 (c) Fraction of experimentally determined “floaters” and “sinkers” as a function of dust load per colony.
279 Pictures show typical dust loads as quantified through image analysis.

280 3.1.2 Effect of dust on colony sinking velocity

281 Initial sinking velocities for individual colonies were examined three times: without any dust, with
282 medium dust load (20 to 1400 ng colony⁻¹), and with high dust load (330 to 4400 ng colony⁻¹).
283 Experiments were repeated on five different days obtaining 75 data pairs of dust loads and sinking
284 velocities (Table S2). As before, colonies were imaged prior to and after each step to track their
285 actual dust loads. Data from two representative days (October 18th & 20th 2020) with six individual
286 colonies show that moderate dust load of 100-400 ng did not affect the colony’s sinking velocity,
287 which remained at 40-50 m·d⁻¹ (Fig. 2a). The initial colony sinking velocities at these low dust loads
288 were presumably controlled by colony size, colony composition (i.e. carbohydrate content) and gas
289 vesicles but not by dust (Held et al., 2022; Walsby, 1992), a region which we term “colony-
290 controlled” (Fig. 2, yellow area). This region is typified by the lack of effect of dust on the initial
291 colony sinking velocity and is in-line with our other observations from the sedimentation chambers
292 after 15 min (Fig. 1). Combined with field observations (Fig. 1a), our results suggest that Red Sea
293 colonies can maintain their buoyancy when interacting with several hundred nanograms of dust.

294 Further dust addition (1-4 µg per colony) shifted the measured sinking velocities into a dust-
295 controlled region (Fig 2, blue area). In this region, sinking velocities increased linearly with the
296 colony’s dust load (Fig. 2b). A linear relationship is expected based on theoretical considerations
297 (Stoke’s law) and direct sinking velocity measurements of size-specific ballasted aggregates (Engel
298 et al., 2009; Iversen & Ploug, 2010). However, according to Stoke’s law, sinking velocity is impacted
299 by both aggregate size and density (e.g. Laurenceau-Cornec et al., 2020). In our case, the colony size
300 remained unchanged for all dust loads since it was centered within the colony core (as confirmed
301 by microscopic observations). Taking into consideration the colony volume and density and the
302 centered dust we derived a linear relationship between dust load and colony sinking velocity (Eq. 1),
303 that should apply for the blue region (see methods and supplementary text S1 and S2). This
304 theoretical calculation predicted a slope (K) of 0.02-0.06 m·d⁻¹·ng⁻¹, implying that 100 ng dust will

305 increase the colony sinking velocity by 2-6 meters per day. Our experimental data yielded a slope (K)
306 of $0.06 \text{ m}\cdot\text{d}^{-1}\cdot\text{ng}^{-1}$ (Fig. 2b) very similar to these theoretical predictions and thus supports our
307 experimental approach. The match between experiments and predictions holds for dust-loaded
308 colonies but not for dust-free colonies. Our measured sinking velocities of particle-free colonies
309 ($40\text{-}55 \text{ m}\cdot\text{d}^{-1}$, Fig. 2) exceed their predicted sinking velocities ($0\text{-}9 \text{ m}\cdot\text{d}^{-1}$, Table S5). Yet, this
310 mismatch may be explained by *Trichodesmium*'s ability to modify their density (Romans et al., 1994;
311 Tracy A. Villareal & Carpenter, 1990).

312 The sinking velocities measured ($20\text{-}60 \text{ m}\cdot\text{d}^{-1}$) for particle-free colonies (Fig. 2) compare well with
313 those of Walsby (1978), who experimentally observed maximal sinking velocities of $60 \text{ m}\cdot\text{d}^{-1}$ for
314 natural *Trichodesmium thiebautii* from the Sargasso and Caribbean Sea. The vertical motion of
315 *Trichodesmium* has been reported early-on (J. Kromkamp & Walsby, 1992; T. A. Villareal &
316 Carpenter, 2003), and draws large interest in terms of carbon export to depth (Bonnet et al., 2023),
317 and fueling of the deep ocean with fixed nitrogen (Benavides et al., 2022). Such vertical migration
318 was hypothesized to provide an ecological advantage to *Trichodesmium* and enable it to mine
319 phosphorus from the thermocline (Karl et al., 1992; White et al., 2006). Sinking of *Trichodesmium*
320 colonies can occur through gravitational sinking or downwelling events (Guidi et al., 2012), both of
321 which can further be accelerated by mineral ballasting (Pabortsava et al., 2017) or sudden
322 autocatalytic cell death in response to nutrient limitation (Berman-Frank et al., 2004). Our study is
323 the first to experimentally quantify the effect of dust on the colony's sinking velocity, and our
324 findings conform to theoretical predictions, modelling data and *in situ* observations (Laurenceau-
325 Cornec et al., 2020; Walsby, 1978; White et al., 2006). To conclude, our experiments show that
326 *Trichodesmium* colonies can control their buoyancy even when loaded with up to 300-400 ng dust
327 and that collection of $1 \mu\text{g}$ dust will slightly increase their sinking velocity by $\sim 60 \text{ m}\cdot\text{d}^{-1}$.

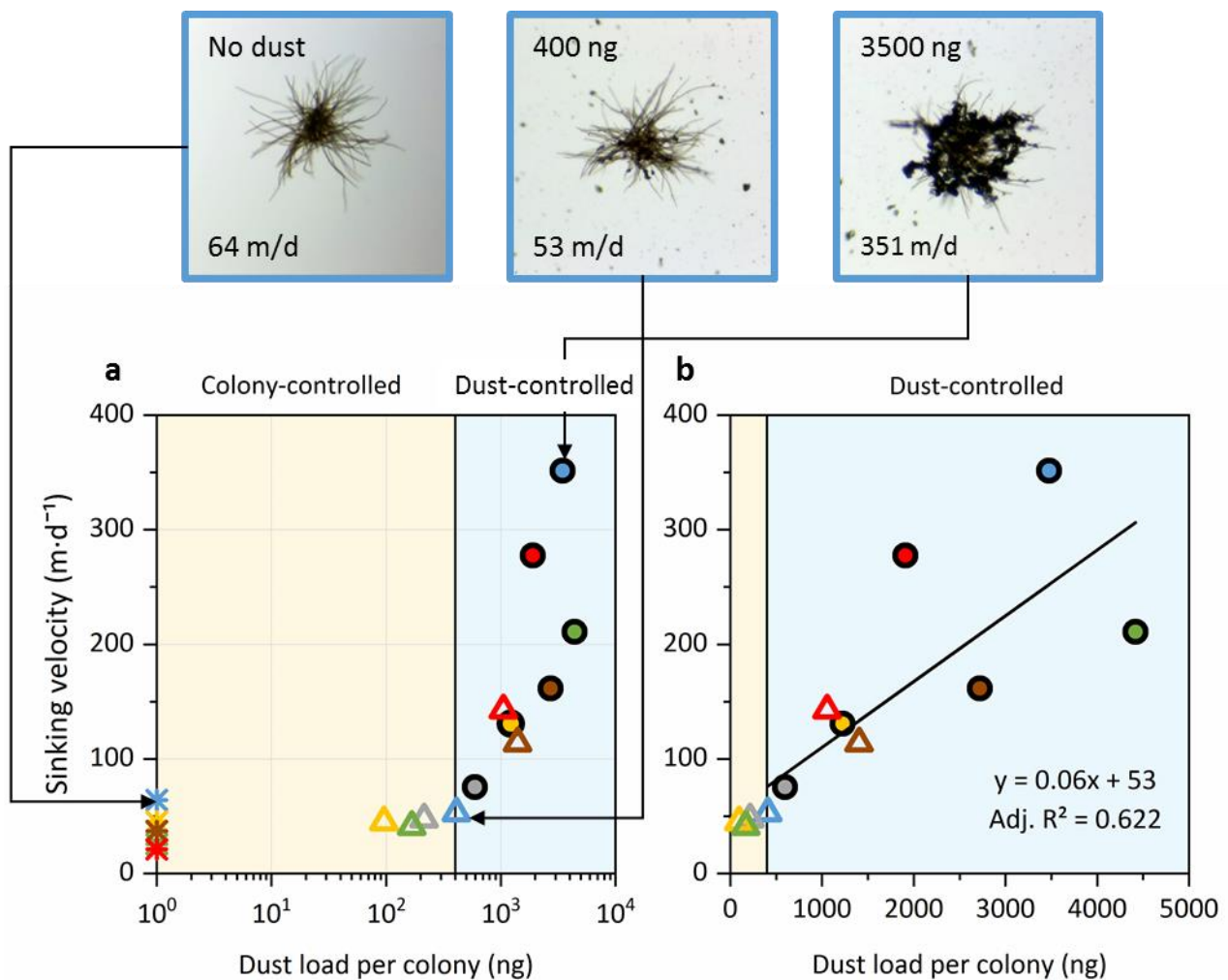


Figure 2. Effect of dust load on sinking velocities of Rea Sea *T. thiebautii* colonies.

(a) Sinking velocities of six individual colonies each measured repeatedly with increasing dust loads and labeled with a distinct color. Sinking velocities of particle-free colonies are noted by stars, colonies with medium dust load by triangles and colonies with high dust load by circles. Two regions were identified: colony-controlled area (yellow shaded) and dust-controlled area (blue shaded). Images above show the increasing dust loads of a single colony (blue-labeled).

(b) Zoom in on the dust-controlled zone, where sinking velocity increased linearly with dust load, at a slope (K) that matched theoretical calculations (see text).

3.1.3 Effect of dust loss on colony sinking velocity

During sedimentation experiments a significant loss of particles from most colonies (42 out of 50 total data pairs) was observed, especially from the heavily-loaded ones. Comparing colony images taken prior to and after the experiments, a loss of 10 ng - 3 µg dust per colony was calculated (Table S6). This massive loss of dust is expected to decrease the sinking velocity of colonies if the loss occurred in early stages of the experiment. Seeking to illustrate this effect, several representative

colonies were plotted in Fig. 3 (see supplementary text S3 for the selection criterion) were compared to the linear relationship established in Fig. 2b ($y = 0.06 \text{ m}\cdot\text{d}^{-1}\cdot\text{ng}^{-1} \times \text{dust weight (ng)} + 53 \text{ m}\cdot\text{d}^{-1}$). All these colonies plot below their expected sinking velocities noted by the black line, indicating that dust was lost during the experiment and decreased their sinking velocities (Fig. 3a). Replotting the measured sinking velocities of these colonies against their final dust loads (Fig. 3b), yield values that are nearer to the line. Thus, it seems that these colonies were sinking at velocities that match the final dust loads, probably since this loss occurred at the beginning of the experiment. Such analysis, made possible by the relationship established in this study, revealed that dust loss can decrease the colony sinking velocity in a predictable manner.

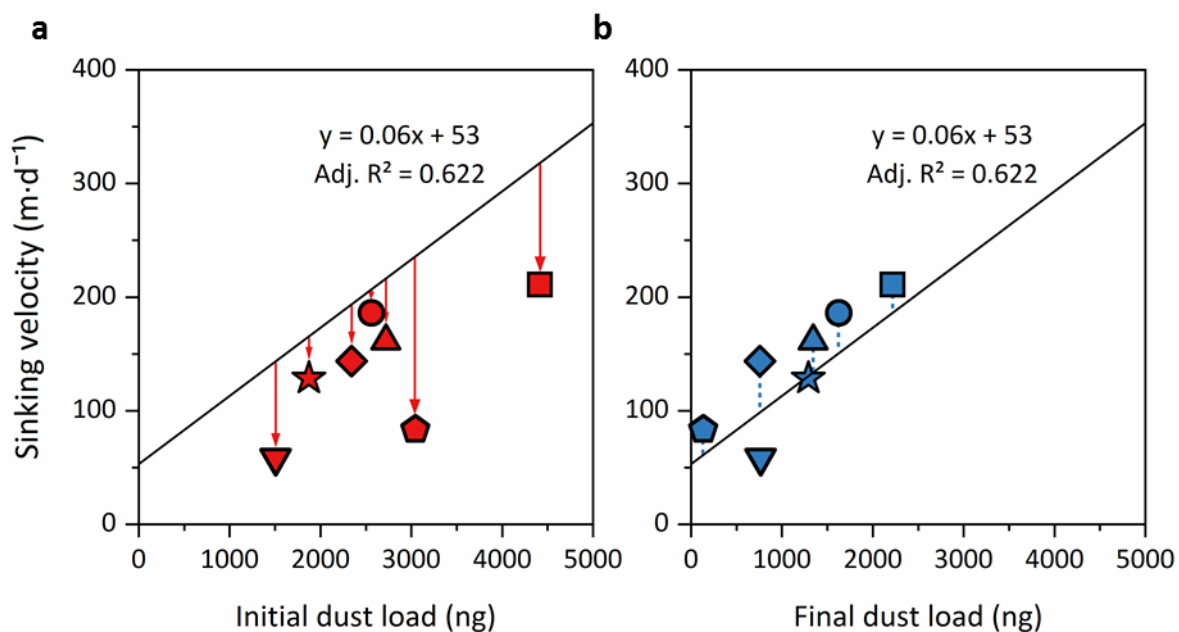


Figure 3. Effect of dust loss on colony sinking velocity.

Measured sinking velocities of seven representative colonies (shown as different symbols) plotted against their initial (a) and final (b) dust loads. The equation (black line) is the linear relationship established in Fig. 2b. Arrows and dash lines indicate the mismatch of measured sinking velocities and expected velocities calculated from initial and final dust loads, respectively. See Fig. S3 for additional colonies.

3.2 Toxic effects of dust on *Trichodesmium*

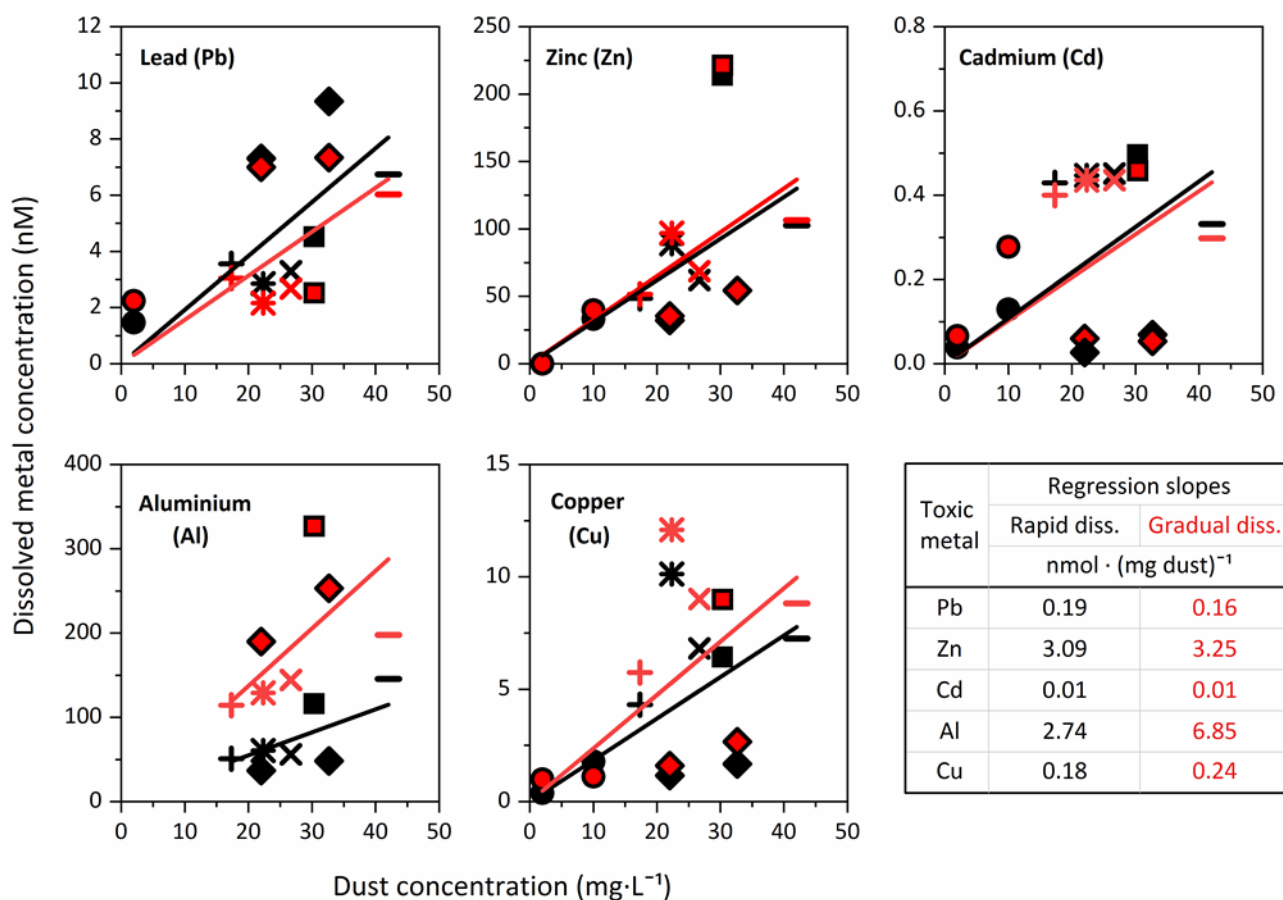
Dust and other aerosols contain an array of toxic elements (Bozlaker et al., 2013). Upon dust deposition on the surface ocean, some elements are rapidly released and may induce toxicity to positively buoyant *Trichodesmium* blooms that accumulate at the surface. Seeking to evaluate the toxicity of dust to *Trichodesmium* blooms, the fraction of rapidly released toxic metals was

measured and the impact of dust leachate on *Trichodesmium* mortality was observed. In addition, colonies that concentrate dust may also experience a continuous flux of toxic metals that are gradually released from the centered particles. The gradual release of metals was hereby measured and the mortality of dust-loaded colonies was examined.

3.2.1 Kinetics of toxic metal release from dust

Toxic metal release to seawater was measured at two dust concentrations and data was gathered according to time, differentiating between rapidly (10 min - 6 h) and gradually (12 h - 7 d) released elements. To contextualize our data, we included additional dissolution measurements conducted by Mackay et al. (2015) resulting in a dissolution dataset composed of seven different dust samples collected from the Gulf of Aqaba over several years (Fig. 4, see Table S7 for additional elements). To enable easy extrapolation to natural conditions, concentrations of dissolved metal released from the different dust samples were plotted against the concentrations of dust used in the experiments. In general, higher dissolved metals were recorded at higher dust concentrations and a linear correlation can be fitted to the data (Fig. 4).

Since *Trichodesmium's* exposure to dust depends on the interaction time, special attention was paid to the timing and release mode of each metal, following the Mackay et al. (2015) scheme. Concentrations of zinc (Zn) and cadmium (Cd) remained constant with time (gradual=rapid, Fig. 4) and hence were considered rapidly released elements. On the other hand, aluminum (Al) and copper (Cu) accumulated with dissolution time (gradual>rapid, Fig. 4), and were considered gradually released elements. Lead (Pb) concentration dropped slightly with time (gradual<rapid, Fig. 4), reflecting its tendency to adsorb onto particles and surfaces (Bruland et al., 2013). Based on these linear slopes and release mode (rapid versus gradual), the “cocktail” of toxic elements released during dust deposition events or within the colony center can be evaluated and linked to the incubation studies with *Trichodesmium*.



387

388 **Figure 4. Compilation of dust dissolution experiments conducted in seawater using different dust**
 389 **samples and concentrations.**

390 The dataset combines new measurements (circles) and published data from (Mackey et al., 2015) and
 391 includes seven dust samples plotted as different symbols. Metal release kinetics is presented by two
 392 categories - rapidly released metals (black, up to 6hrs) and gradually released metals (red, up to 7 days).
 393 Regression slopes linking dust and dissolved metal concentrations are plotted and summarized in the table
 394 next to the graph (see Fig. S6 for additional elements).

395 3.2.2 Dust toxicity to *Trichodesmium* – fractions and doses

396 To assess dust toxicity to *Trichodesmium*, ~180 freshly collected natural colonies were incubated
 397 with increasing dust concentrations for 24 hrs and mortality was assessed visually based on colony
 398 integrity and filament degradation (Fig. S4). To distinguish between the toxic effects of rapidly and
 399 gradually released metals, colonies were exposed to dust leachate and raw dust, respectively
 400 (where the leachate was obtained after 10 min from dust addition to seawater).

401 Incubating *Trichodesmium* with 2 and 10 mg·L⁻¹ dust resulted in negligible mortality of only one or
402 two of the 16 colonies incubated (red and blue lines in Fig. 5a and 5b). These dust loads are within
403 the range reported for natural dust storms (<10 mg·L⁻¹, Ren et al., 2011; Zhang et al., 2019), and
404 hence dust load from such storms are not predicted to induce *Trichodesmium* mortality. Low
405 mortality (13%) was observed in colonies incubated with 100 mg·L⁻¹ dust leachate, far below the
406 LC50 toxicity threshold, which is the lethal concentration that results in death of 50% of the
407 colonies (Echeveste et al., 2012). At higher dust concentrations of 500 and 1000 mg·L⁻¹, significant
408 mortality was observed, ranging from 50-90% of the colonies (purple and orange lines in Fig. 5a and
409 Fig. 5b), indicative of acute toxicity. Based on these incubations, we conservatively set the LC50
410 toxicity threshold at 500 mg·L⁻¹ (although it may occur anywhere above 100 mg·L⁻¹).

411 Overall, the mortality of *Trichodesmium* was comparable between the leachate (Fig. 5a) and dust
412 particles (Fig. 5b). This implies that metals released from dust during 10 min are the key
413 contributors to its toxicity to *Trichodesmium*. Utilizing the linear fit from Fig. 4, toxic metals
414 concentrations in each incubation can be estimated (Fig. 5c). For example, in the incubation with
415 500 mg·L⁻¹ dust that yielded 50% mortality, *Trichodesmium* is expected to experience 5 nM Cd, 95
416 nM Pb, 90 nM Cu, and >1 µM of Zn and Al (Fig. 5c). Interestingly, negligible mortality occurred in
417 the 100 mg·L⁻¹ dust leachate incubation, conditions where 1 nM Cd, ~20 nM Pb and Cu, and ~300
418 nM of Zn and Al were predicted (Fig. 5b and 5c). Given the absence of literature data on
419 *Trichodesmium*'s response to a cocktail of toxic metals, it remains inconclusive whether these levels
420 were sub-lethal or *Trichodesmium* was capable of detoxifying these metals. Typically, toxicity
421 thresholds (e.g. effective concentration 50% (EC50s) or lethal concentration 50% (LC50s) are
422 obtained for a single metal, varying amongst phytoplankton types and sizes (Echeveste et al., 2012;
423 Paytan et al., 2009; Yang et al., 2019). To provide context, Cd and Pb toxicity thresholds (LC50s) for
424 natural phytoplankton from different ocean basins were reported to range from 2-4000 nM for Cd,
425 and 100-2000 nM for Pb (Echeveste et al., 2012).

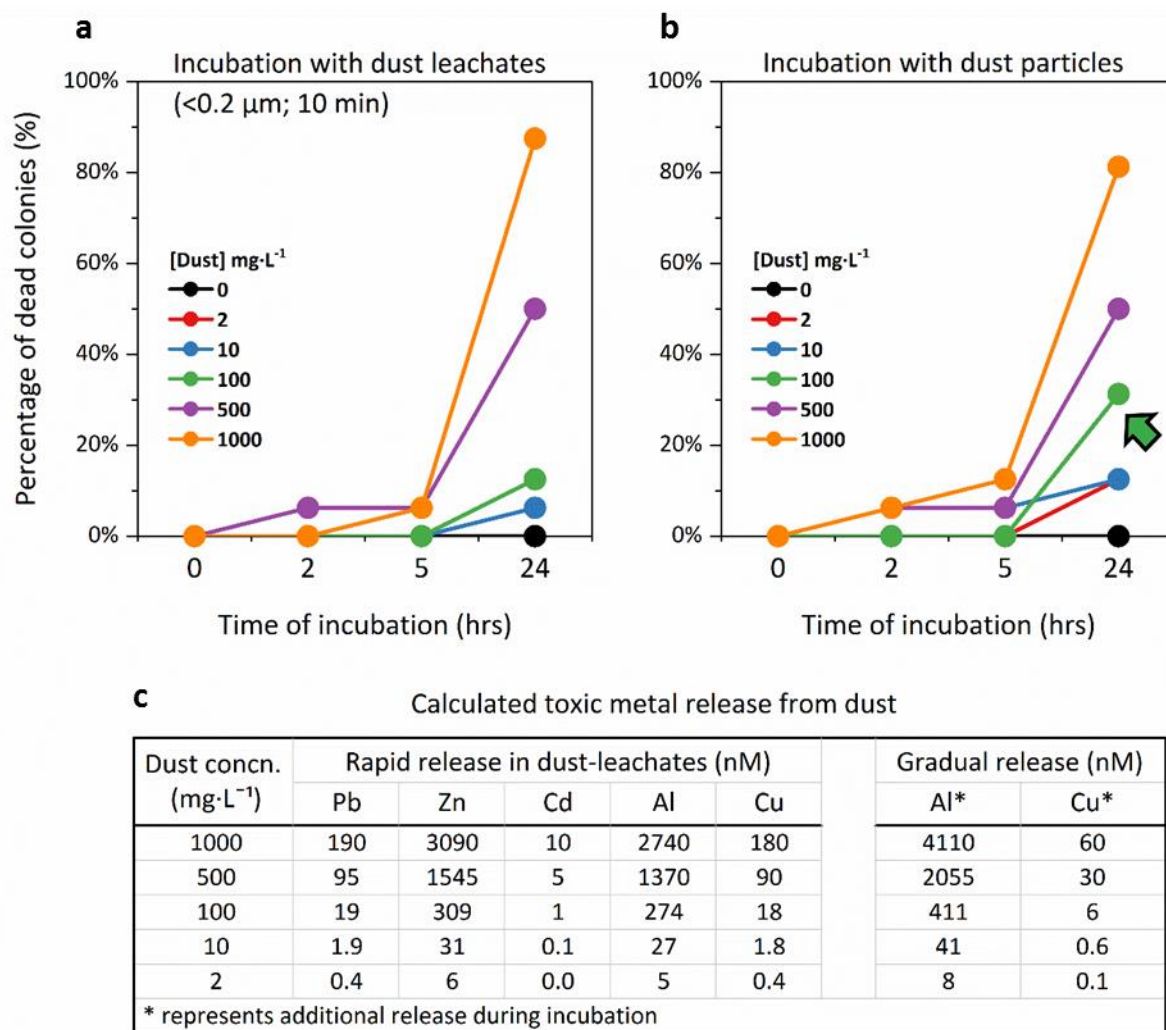


Figure 5. Impact of dust on mortality of Red Sea *Trichodesmium* colonies and estimated toxic metals released during incubations.

Mortality of natural colonies incubated for 24 hrs with increasing concentrations of (a) dust leachate and (b) whole dust. (c). Calculated metal release from dust during the mortality assays based on the regression slopes obtained in Fig. 4. Data was compiled from 2 different experiments. The dust leachate was filtered within 10 min of dust suspension in seawater to represent rapidly released metals, while whole dust provided also gradually released metals. The toxicity of dust leachate and whole dust was comparable at high concentrations, but as indicated by the green arrow, at $100 \text{ mg}\cdot\text{L}^{-1}$ dust, the mortality was higher with whole dust.

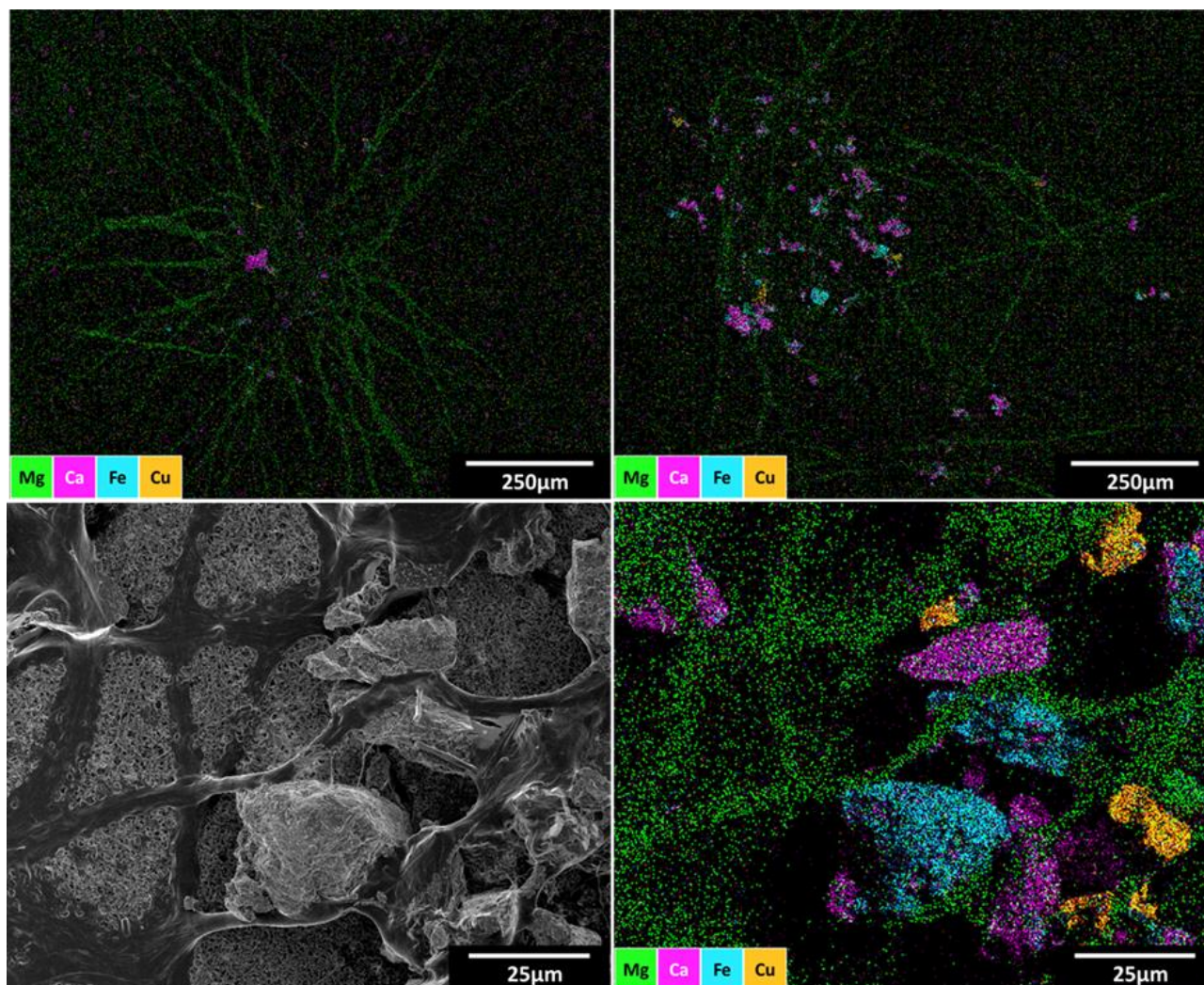
437 A more detailed look at the data shows subtle changes in the mortality of colonies incubated with
438 $100 \text{ mg}\cdot\text{L}^{-1}$ dust leachate compared to the whole dust (green arrow in Fig. 5). At these low dust
439 concentrations (e.g. $100 \text{ mg}\cdot\text{L}^{-1}$), only two colonies died in the leachate (13%), while five colonies
440 died in the whole dust (31%). This added mortality may have originated from the gradually released
441 metals Al and Cu (Fig. 5c). In a parallel set of experiments, we tested the mortality of colonies
442 incubated with increasing Cu concentrations, obtaining 30 and 50% mortality at 5 and 10 nM Cu,
443 respectively (Fig. S5). The estimated gradually release of 0.1-6 nM Cu (Fig. 5c) may hereby explain
444 the elevated mortality in the whole dust incubation, especially when also considering the high
445 levels of Al.

446 Regarding the toxicity of metals in dust-centering colonies, it appears that Pb, Zn and Cd are not a
447 major concern, as these elements are released from dust before they interact with the colonies. But
448 the gradually released elements Al and Cu may cause toxicity to colonies that center dust. As dust is
449 confined within the colony core and the diffusion to the surrounding water is limited, the colony or
450 its core volume should be considered as the relevant volume for metal release. Given $\sim 1 \text{ }\mu\text{L}$ colony
451 volume, dust loads of 0.2-1 μg yield effective dust concentration of $200\text{-}1000 \text{ mg}\cdot\text{L}^{-1}$ (Fig. S7). At
452 these high dust concentrations, high exposure to gradually released Al and Cu is expected (Fig. 5c).
453 The exposure to these metals may be even larger when considering the volume of the colony core
454 where the dissolution occurs and not the entire colony volume. Nonetheless, colonies that
455 accumulated even higher dust loads (1-10 μg) showed no signs of mortality during incubations that
456 lasted 24 hrs (Fig. S8). The survival of colonies with an effective dust load of over $1000 \text{ mg}\cdot\text{L}^{-1}$ and
457 projected high Cu and Al fluxes (Fig. 5c) is intriguing. These observations call for further research
458 measuring metal fluxes within colonies and exploring possible detoxification and physiological
459 defense mechanisms. Such mechanisms may include metal binding by extracellular polymeric
460 substances (EPS) and specific ligands (Gledhill et al., 2019) and metal excretion through efflux
461 proteins (Hewson et al., 2009).

462 3.2.3 Selective removal of Cu minerals

463 Hypothesizing that colonies may try to reduce toxicity through the removal of particles, natural
464 colonies were incubated with Cu-containing minerals (malachite) for 24 hrs. To ensure optimal
465 colony-mineral interactions, the Cu minerals were mixed with Fe minerals (hematite), which are
466 typically preferred by *Trichodesmium*. All colonies interacted strongly with particles throughout the

467 incubation and showed strong preference for the Fe-minerals. Only few colonies contained Cu-
468 minerals, but these were present even at 24 hrs (Fig. 6). The finding of Cu minerals on colonies at
469 the end of the incubation does not support our hypothesis and there is currently no evidence to
470 support the selective removal of toxic minerals.



471

472 **Figure 6. SEM-EDX images of natural *Trichodesmium* colonies incubated with Cu-minerals**
473 **(malachite) and Fe-minerals (hematite).**

474 Probing the ability of *Trichodesmium* to distinguish and selectively remove toxic particles, colonies were
475 incubated with malachite and hematite up to 24 hrs. Several colonies were imaged at different magnification
476 (scale bars within images), showing the presence of both minerals throughout the incubation (Cu – yellow,
477 Fe – blue). *Trichodesmium* was imaged through its magnesium content (green) and the malachite sample
478 also contained calcium (Ca) minerals (pink). See Fig. S10-S13 for additional elemental maps.

479

480 4. Summary

481 Having studied the potential negative effects of dust on natural *Trichodesmium* colonies, we predict
482 that in a typical open-ocean setting, the potential benefit of dust as a nutrient source outweighs the
483 risks of buoyancy loss and toxification. In the Gulf of Aqaba, puff-shaped *T. thiebautii* colonies
484 collected *in situ* were usually observed to contain less than 200 ng of dust per colony, which is
485 below the threshold where sinking velocity becomes dust-controlled (Fig. 1) and is insufficient to
486 induce toxicity through metal release (Fig. 5). In other environments (e.g. coastal seas, Mackey et
487 al., 2012), however, *Trichodesmium* may encounter more toxic aerosols and the concepts laid here
488 may facilitate the evaluation of those risks. With regards to buoyancy, accelerated sinking velocities
489 due to interactions with dust may be significant to C export, and may help explain recent
490 measurements of active N₂ fixation by *Trichodesmium* at 1000 meters (Benavides et al., 2022). If
491 indeed colonies can modulate their particle load, the dust-induced sinking may
492 benefit *Trichodesmium* and expand its ecological niche.

493

494 Author contributions

495 **Conceptualization:** Siyuan Wang, Yeala Shaked

496 **Data curation:** Siyuan Wang

497 **Formal analysis:** Siyuan Wang, Futing Zhang, Coco Koedooder, Odeta Qafoku, Subhajit Basu,
498 Stephan Krisch, Anna-Neva Visser, Meri Eichner, Nivi Kessler

499 **Methodology:** Siyuan Wang, Futing Zhang, Odeta Qafoku, Subhajit Basu, Stephan Krisch, Anna-
500 Neva Visser

501 **Funding acquisition:** Rene M. Boiteau, Martha Gledhill, Yeala Shaked

502 **Supervision:** Yeala Shaked

503 **Writing – original draft:** Siyuan Wang, Yeala Shaked

504 **Writing – review & editing:** Futing Zhang, Coco Koedooder, Odeta Qafoku, Subhajit Basu, Stephan
505 Krisch, Anna-Neva Visser, Meri Eichner, Nivi Kessler, Rene M. Boiteau, Martha Gledhill

506

507 Acknowledgements

508 We extend our sincere gratitude to Murielle Dray (IUI) and Emanuel Sestieri (IUI) for their
509 invaluable assistance during this study. We appreciate the Mineral collection at the National
510 Natural History Collections at the Hebrew University for donating the mineral specimens (hematite)
511 used in this work. Siyuan Wang thanks Prof. Angelicque E. White for her insightful suggestions
512 regarding the model of sinking velocity and to Mr. Antonio Colussi and Dr. Lina Sakhneny for their
513 contributions to colony collection and toxicity assays. This study was funded by ISF-NSFC joint
514 research program (Grant No. 2398/18) and ISF (260/21). Siyuan Wang acknowledges CSC-HUJI
515 doctoral fellowship and Futing Zhang acknowledges PBC Postdoctoral fellowship.

516

517 **Conflict of interest**

518 The authors declare that they have no conflict of interest.

519

520 **Data availability statement**

521 Data generated for this study were uploaded as supplementary materials. All python codes for
522 sinking velocity can be found in Github (<https://github.com/Zhanzhu1110/Trichobuoyancy.git>) and
523 in Zenodo (<https://zenodo.org/records/10290901>; DOI:10.5281/zenodo.10290901)(Wang et al.,
524 2023). Data of metal release (dust concentrations = 17-42 mg·L⁻¹) are available from Mackay et al.
525 (2015), and a complete supplementary data file is also provided herein for ease of access.

526

527 Reference

- 528 Anderson, O. R. (1977). Fine Structure of a Marine Ameba Associated with a Blue-Green Alga in the
529 Sargasso Sea. *The Journal of Protozoology*, 24(3), 370–376.
530 <https://doi.org/10.1017/cbo9780511600586.003>
- 531 Basu, S., & Shaked, Y. (2018). Mineral iron utilization by natural and cultured *Trichodesmium* and
532 associated bacteria. *Limnology and Oceanography*, 63(6), 2307–2320.
533 <https://doi.org/10.1002/lno.10939>
- 534 Basu, S., Gledhill, M., de Beer, D., Prabhu Matondkar, S. G., & Shaked, Y. (2019). Colonies of marine
535 cyanobacteria *Trichodesmium* interact with associated bacteria to acquire iron from dust.
536 *Communications Biology*, 2(1), 1–8. <https://doi.org/10.1038/s42003-019-0534-z>
- 537 Benaltabet, T., Lapid, G., & Torfstein, A. (2022). Dissolved aluminium dynamics in response to dust
538 storms, wet deposition, and sediment resuspension in the Gulf of Aqaba, northern Red Sea.
539 *Geochimica et Cosmochimica Acta*, 335, 137–154. <https://doi.org/10.1016/j.gca.2022.08.029>
- 540 Benavides, M., Bonnet, S., Le Moigne, F. A. C., Armin, G., Inomura, K., Hallstrøm, S., et al. (2022).
541 Sinking *Trichodesmium* fixes nitrogen in the dark ocean. *ISME Journal*, 16(10), 2398–2405.
542 <https://doi.org/10.1038/s41396-022-01289-6>
- 543 Berman-Frank, I., Bidle, K. D., Haramaty, L., & Falkowski, P. G. (2004). The demise of the marine
544 cyanobacterium, *Trichodesmium* spp., via an autocatalyzed cell death pathway. *Limnology and*
545 *Oceanography*, 49(4 I), 997–1005. <https://doi.org/10.4319/lo.2004.49.4.0997>
- 546 Bif, M. B., & Yunes, J. S. (2017). Distribution of the marine cyanobacteria *Trichodesmium* and their
547 association with iron-rich particles in the South Atlantic Ocean. *Aquatic Microbial Ecology*,
548 78(2), 107–119. <https://doi.org/10.3354/ame01810>
- 549 Bonnet, S., Benavides, M., Le Moigne, F. A. C., Camps, M., Torremocha, A., Grosso, O., et al. (2023).
550 Diazotrophs are overlooked contributors to carbon and nitrogen export to the deep ocean.
551 *ISME Journal*, 17(1), 47–58. <https://doi.org/10.1038/s41396-022-01319-3>
- 552 Bozlaker, A., Prospero, J. M., Fraser, M. P., & Chellam, S. (2013). Quantifying the contribution of
553 long-range saharan dust transport on particulate matter concentrations in Houston, Texas,

554 using detailed elemental analysis. *Environmental Science and Technology*, 47(18), 10179–
555 10187. <https://doi.org/10.1021/es4015663>

556 Bruland, K. W., Middag, R., & Lohan, M. C. (2013). *Controls of Trace Metals in Seawater. Treatise on*
557 *Geochemistry: Second Edition* (2nd ed., Vol. 8). Elsevier Ltd. [https://doi.org/10.1016/B978-0-](https://doi.org/10.1016/B978-0-08-095975-7.00602-1)
558 08-095975-7.00602-1

559 Capone, D. G., Zehr, J. P., Paerl, H. W., Bergman, B., & Carpenter, E. J. (1997). *Trichodesmium*, a
560 globally significant marine cyanobacterium. *Science*, 276(5316), 1221–1229.
561 <https://doi.org/10.1126/science.276.5316.1221>

562 Cerdan-Garcia, E., Baylay, A., Polyviou, D., Woodward, E. M. S., Wrightson, L., Mahaffey, C., et al.
563 (2022). Transcriptional responses of *Trichodesmium* to natural inverse gradients of Fe and P
564 availability. *ISME Journal*, 16(4), 1055–1064. <https://doi.org/10.1038/s41396-021-01151-1>

565 Chen, Y., Tovar-Sanchez, A., Siefert, R. L., Sañudo-Wilhelmy, S. A., & Zhuang, G. (2011). Luxury
566 uptake of aerosol iron by *Trichodesmium* in the western tropical North Atlantic. *Geophysical*
567 *Research Letters*, 38(18). <https://doi.org/10.1029/2011GL048972>

568 Echeveste, P., Agustí, S., & Tovar-Sánchez, A. (2012). Toxic thresholds of cadmium and lead to
569 oceanic phytoplankton: Cell size and ocean basin-dependent effects. *Environmental Toxicology*
570 *and Chemistry*, 31(8), 1887–1894. <https://doi.org/10.1002/etc.1893>

571 Eichner, M., Inomura, K., Pierella Karlusich, J. J., & Shaked, Y. (2023). Better together? Lessons on
572 sociality from *Trichodesmium*. *Trends in Microbiology*, xx(xx), 1–13.
573 <https://doi.org/10.1016/j.tim.2023.05.001>

574 Engel, A., Szlosek, J., Abramson, L., Liu, Z., & Lee, C. (2009). Investigating the effect of ballasting by
575 CaCO₃ in *Emiliania huxleyi*: I. Formation, settling velocities and physical properties of
576 aggregates. *Deep-Sea Research Part II: Topical Studies in Oceanography*, 56(18), 1396–1407.
577 <https://doi.org/10.1016/j.dsr2.2008.11.027>

578 Frischkorn, K. R., Haley, S. T., & Dyhrman, S. T. (2018). Coordinated gene expression between
579 *Trichodesmium* and its microbiome over day-night cycles in the North Pacific Subtropical Gyre.
580 *ISME Journal*, 12(4), 997–1007. <https://doi.org/10.1038/s41396-017-0041-5>

581 Gledhill, M., Basu, S., & Shaked, Y. (2019). Metallophores associated with: *Trichodesmium*
582 erythraeum colonies from the Gulf of Aqaba. *Metallomics*, 11(9), 1547–1557.
583 <https://doi.org/10.1039/c9mt00121b>

584 Guidi, L., Calil, P. H. R., Duhamel, S., Björkman, K. M., Doney, S. C., Jackson, G. A., et al. (2012). Does
585 eddy-eddy interaction control surface phytoplankton distribution and carbon export in the
586 North Pacific Subtropical Gyre? *Journal of Geophysical Research: Biogeosciences*, 117(2), 1–12.
587 <https://doi.org/10.1029/2012JG001984>

588 Guo, C., Zhou, Y., Zhou, H., Su, C., & Kong, L. (2022). Aerosol Nutrients and Their Biological Influence
589 on the Northwest Pacific Ocean (NWPO) and Its Marginal Seas. *Biology*, 11(6), 1–18.
590 <https://doi.org/10.3390/biology11060842>

591 Held, N. A., Webb, E. A., McIlvin, M. M., Hutchins, D. A., Cohen, N. R., Moran, D. M., et al. (2020).
592 Co-occurrence of Fe and P stress in natural populations of the marine diazotroph
593 *Trichodesmium*. *Biogeosciences*, 17(9), 2537–2551. <https://doi.org/10.5194/bg-17-2537-2020>

594 Held, N. A., Sutherland, K. M., Webb, E. A., McIlvin, M. R., Cohen, N. R., Devaux, A. J., et al. (2021).
595 Mechanisms and heterogeneity of *in situ* mineral processing by the marine nitrogen fixer
596 *Trichodesmium* revealed by single-colony metaproteomics. *ISME Communications*, 1(1), 1–9.
597 <https://doi.org/10.1038/s43705-021-00034-y>

598 Held, N. A., Waterbury, J. B., Webb, E. A., Kellogg, R. M., McIlvin, M. R., Jakuba, M., et al. (2022).
599 Dynamic diel proteome and daytime nitrogenase activity supports buoyancy in the
600 cyanobacterium *Trichodesmium*. *Nature Microbiology*, 7(2), 300–311.
601 <https://doi.org/10.1038/s41564-021-01028-1>

602 Hewson, I., Poretsky, R. S., Dyhrman, S. T., Zielinski, B., White, A. E., Tripp, H. J., et al. (2009).
603 Microbial community gene expression within colonies of the diazotroph, *Trichodesmium*, from
604 the Southwest Pacific Ocean. *ISME Journal*, 3(11), 1286–1300.
605 <https://doi.org/10.1038/ismej.2009.75>

606 Iversen, M. H., & Ploug, H. (2010). Ballast minerals and the sinking carbon flux in the ocean: Carbon-
607 specific respiration rates and sinking velocity of marine snow aggregates. *Biogeosciences*, 7(9),
608 2613–2624. <https://doi.org/10.5194/bg-7-2613-2010>

609 Karl, D. M., Letelier, R., Hebel, D. V., Bird, D. F., & Winn, C. D. (1992). *Trichodesmium* blooms and
610 new nitrogen in the North Pacific gyre. In J. G. Carpenter, E.J., Capone, D.G., Rueter (Ed.),
611 *Marine pelagic cyanobacteria* (pp. 219–237). Springer, Dordrecht.
612 https://doi.org/10.1007/978-94-015-7977-3_14

613 Kessler, N., Kraemer, S. M., Shaked, Y., & Schenkeveld, W. D. C. (2020). Investigation of
614 Siderophore-Promoted and Reductive Dissolution of Dust in Marine Microenvironments Such
615 as *Trichodesmium* Colonies. *Frontiers in Marine Science*, 7(March), 1–15.
616 <https://doi.org/10.3389/fmars.2020.00045>

617 Kessler, N., Armoza-Zvuloni, R., Wang, S., Basu, S., Weber, P. K., Stuart, R. K., & Shaked, Y. (2020).
618 Selective collection of iron-rich dust particles by natural *Trichodesmium* colonies. *ISME Journal*,
619 14(1), 91–103. <https://doi.org/10.1038/s41396-019-0505-x>

620 Koedooder, C., Landou, E., Zhang, F., Wang, S., Basu, S., Berman-Frank, I., et al. (2022).
621 Metagenomes of Red Sea Subpopulations Challenge the Use of Marker Genes and Morphology
622 to Assess *Trichodesmium* Diversity. *Frontiers in Microbiology*, 13(May).
623 <https://doi.org/10.3389/fmicb.2022.879970>

624 Krisch, S., Hopwood, M. J., Roig, S., Gerringa, L. J. A., Middag, R., Rutgers van der Loeff, M. M., et al.
625 (2022). Arctic – Atlantic Exchange of the Dissolved Micronutrients Iron, Manganese, Cobalt,
626 Nickel, Copper and Zinc With a Focus on Fram Strait. *Global Biogeochemical Cycles*, 36(5).
627 <https://doi.org/10.1029/2021GB007191>

628 Kromkamp, J., & Walsby, A. E. (1992). Buoyancy regulation and vertical migration of *Trichodesmium*:
629 a computer-model prediction. In J. G. Carpenter, E.J., Capone, D.G., Rueter (Ed.), *Marine*
630 *Pelagic Cyanobacteria: Trichodesmium and other Diazotrophs* (pp. 239–248). Springer,
631 Dordrecht. https://doi.org/10.1007/978-94-015-7977-3_15

632 Kromkamp, Jacco, & Walsby, A. E. (1990). A computer model of buoyancy and vertical migration in
633 cyanobacteria. *Journal of Plankton Research*, 12(1), 161–183.
634 <https://doi.org/10.1093/plankt/12.1.161>

635 Laurenceau-Cornec, E. C., Le Moigne, F. A. C., Gallinari, M., Moriceau, B., Toullec, J., Iversen, M. H.,
636 et al. (2020). New guidelines for the application of Stokes’ models to the sinking velocity of

637 marine aggregates. *Limnology and Oceanography*, 65(6), 1264–1285.
638 <https://doi.org/10.1002/lno.11388>

639 Lee, M. D., Walworth, N. G., McParland, E. L., Fu, F. X., Mincer, T. J., Levine, N. M., et al. (2017). The
640 *Trichodesmium* consortium: Conserved heterotrophic co-occurrence and genomic signatures
641 of potential interactions. *ISME Journal*, 11(8), 1813–1824.
642 <https://doi.org/10.1038/ismej.2017.49>

643 Mackey, K. R. M., Buck, K. N., Casey, J. R., Cid, A., Lomas, M. W., Sohrin, Y., & Paytan, A. (2012).
644 Phytoplankton responses to atmospheric metal deposition in the coastal and open-ocean
645 Sargasso Sea. *Frontiers in Microbiology*, 3(OCT), 1–15.
646 <https://doi.org/10.3389/fmicb.2012.00359>

647 Mackey, K. R. M., Chien, C. Te, Post, A. F., Saito, M. A., & Paytan, A. (2015). Rapid and gradual
648 modes of aerosol trace metal dissolution in seawater. *Frontiers in Microbiology*, 6(JAN), 1–11.
649 <https://doi.org/10.3389/fmicb.2014.00794>

650 Mahowald, N. M., Hamilton, D. S., Mackey, K. R. M., Moore, J. K., Baker, A. R., Scanza, R. A., & Zhang,
651 Y. (2018). Aerosol trace metal leaching and impacts on marine microorganisms. *Nature*
652 *Communications*, 9(1). <https://doi.org/10.1038/s41467-018-04970-7>

653 McConnell, C. L., Highwood, E. J., Coe, H., Formenti, P., Anderson, B., Osborne, S., et al. (2008).
654 Seasonal variations of the physical and optical characteristics of saharan dust: Results from the
655 dust outflow and deposition to the ocean (DODO) experiment. *Journal of Geophysical Research*,
656 113, 1–19. <https://doi.org/10.1029/2007JD009606>

657 Mills, M. M., Ridame, C., Davey, M., La Roche, J., & Geider, R. J. (2004). Iron and phosphorus co-
658 limit nitrogen fixation in the eastern tropical North Atlantic. *Nature*, 429(6989), 292–294.
659 <https://doi.org/10.1038/nature03632>

660 Pabortsava, K., Lampitt, R. S., Benson, J., Crowe, C., McLachlan, R., Le Moigne, F. A. C., et al. (2017).
661 Carbon sequestration in the deep Atlantic enhanced by Saharan dust. *Nature Geoscience*, 10(3),
662 189–194. <https://doi.org/10.1038/ngeo2899>

663 Paytan, A., Mackey, K. R. M., Chen, Y., Lima, I. D., Doney, S. C., Mahowald, N., et al. (2009). Toxicity
664 of atmospheric aerosols on marine phytoplankton. *Proceedings of the National Academy of*

665 *Sciences of the United States of America*, 106(12), 4601–4605.
 666 <https://doi.org/10.1073/pnas.0811486106>

667 Polyviou, D., Baylay, A. J., Hitchcock, A., Robidart, J., Moore, C. M., & Bibby, T. S. (2018). Desert dust
 668 as a source of iron to the globally important diazotroph *Trichodesmium*. *Frontiers in*
 669 *Microbiology*, 8(JAN), 1–12. <https://doi.org/10.3389/fmicb.2017.02683>

670 Rapp, I., Schlosser, C., Rusiecka, D., Gledhill, M., & Achterberg, E. P. (2017). Automated
 671 preconcentration of Fe, Zn, Cu, Ni, Cd, Pb, Co, and Mn in seawater with analysis using high-
 672 resolution sector field inductively-coupled plasma mass spectrometry. *Analytica Chimica Acta*,
 673 976, 1–13. <https://doi.org/10.1016/j.aca.2017.05.008>

674 Ren, J. L., Zhang, G. L., Zhang, J., Shi, J. H., Liu, S. M., Li, F. M., et al. (2011). Distribution of dissolved
 675 aluminum in the Southern Yellow Sea: Influences of a dust storm and the spring bloom. *Marine*
 676 *Chemistry*, 125(1–4), 69–81. <https://doi.org/10.1016/j.marchem.2011.02.004>

677 Romans, K. M., Carpenter, E. J., & Bergman, B. (1994). Buoyancy regulation in the colonial
 678 diazotrophic cyanobacterium *Trichodesmium tenue*: ultrastructure and storage of
 679 carbohydrate, polyphosphate, and nitrogen. *Journal of Phycology*, 30(6), 935–942.

680 Rouco, M., Haley, S. T., & Dyhrman, S. T. (2016). Microbial diversity within the *Trichodesmium*
 681 holobiont. *Environmental Microbiology*, 18(12), 5151–5160. [https://doi.org/10.1111/1462-](https://doi.org/10.1111/1462-2920.13513)
 682 [2920.13513](https://doi.org/10.1111/1462-2920.13513)

683 Rubin, M., Berman-Frank, I., & Shaked, Y. (2011). Dust- and mineral-iron utilization by the marine
 684 dinitrogen-fixer *Trichodesmium*. *Nature Geoscience*, 4(8), 529–534.
 685 <https://doi.org/10.1038/ngeo1181>

686 Rueter, J. G., McCarthy, J. J., & Carpenter, E. J. (1979). The toxic effect of copper on *Oscillatoria*
 687 (*Trichodesmium*) *thiebautii*. *Limnology and Oceanography*, 24(3), 558–562.
 688 <https://doi.org/10.4319/lo.1979.24.3.0558>

689 Schladitz, A., Müller, T., Kaaden, N., Massling, A., Kandler, K., Ebert, M., et al. (2009). *In situ*
 690 measurements of optical properties at Tinfou (Morocco) during the Saharan Mineral Dust
 691 Experiment SAMUM 2006. *Tellus, Series B: Chemical and Physical Meteorology*, 61(1), 64–78.
 692 <https://doi.org/10.1111/j.1600-0889.2008.00397.x>

693 Shaked, Y., & Lis, H. (2012). Disassembling iron availability to phytoplankton. *Frontiers in*
694 *Microbiology*, 3(APR), 1–26. <https://doi.org/10.3389/fmicb.2012.00123>

695 Shaked, Y., de Beer, D., Wang, S., Zhang, F., Visser, A. N., Eichner, M., & Basu, S. (2023). Co-
696 acquisition of mineral-bound iron and phosphorus by natural *Trichodesmium* colonies.
697 *Limnology and Oceanography*, 1–14. <https://doi.org/10.1002/lno.12329>

698 Stockdale, A., Krom, M. D., Mortimer, R. J. G., Benning, L. G., Carslaw, K. S., Herbert, R. J., et al.
699 (2016). Understanding the nature of atmospheric acid processing of mineral dusts in supplying
700 bioavailable phosphorus to the oceans. *Proceedings of the National Academy of Sciences of the*
701 *United States of America*, 113(51), 14639–14644. <https://doi.org/10.1073/pnas.1608136113>

702 Tang, W., Cerdán-García, E., Berthelot, H., Polyviou, D., Wang, S., Baylay, A., et al. (2020). New
703 insights into the distributions of nitrogen fixation and diazotrophs revealed by high-resolution
704 sensing and sampling methods. *ISME Journal*, 14(10), 2514–2526.
705 <https://doi.org/10.1038/s41396-020-0703-6>

706 Villareal, T. A., & Carpenter, E. J. (2003). Buoyancy regulation and the potential for vertical
707 migration in the oceanic cyanobacterium *Trichodesmium*. *Microbial Ecology*, 45(1), 1–10.
708 <https://doi.org/10.1007/s00248-002-1012-5>

709 Villareal, Tracy A., & Carpenter, E. J. (1990). Diel buoyancy regulation in the marine diazotrophic
710 cyanobacterium *Trichodesmium thiebautii*. *Limnology and Oceanography*, 35(8), 1832–1837.
711 <https://doi.org/10.4319/lo.1990.35.8.1832>

712 Walsby, A. E. (1978). The properties and buoyancy-providing role of gas vacuoles in *Trichodesmium*
713 Ehrenberg. *British Phycological Journal*, 13(2), 103–116.
714 <https://doi.org/10.1080/00071617800650121>

715 Walsby, A. E. (1992). The gas vesicles and buoyancy of *Trichodesmium*. In J. G. Carpenter, E.J.,
716 Capone, D.G., Rueter (Ed.), *Marine Pelagic Cyanobacteria: Trichodesmium and other*
717 *Diazotrophs* (pp. 141–161). Springer, Dordrecht. [https://doi.org/10.1007/978-94-015-7977-](https://doi.org/10.1007/978-94-015-7977-3_9)
718 [3_9](https://doi.org/10.1007/978-94-015-7977-3_9)

719 Wang, S., Koedooder, C., Zhang, F., Kessler, N., Eichner, M., Shi, D., & Shaked, Y. (2022). Colonies of
720 the marine cyanobacterium *Trichodesmium* optimize dust utilization by selective collection

721 and retention of nutrient-rich particles. *IScience*, 25(1), 103587.
722 <https://doi.org/10.1016/j.isci.2021.103587>

723 Wang, S., Zhang, F., Koedooder, C., Qafoku, O., Basu, S., Krisch, S., et al. (2023). Calculations and
724 simulations of dust factor (K) and sinking velocity of particle-free *Trichodesmium* colonies (v0).
725 *Zenodo*. <https://doi.org/10.5281/zenodo.10290901>

726 White, A. E., Spitz, Y. H., & Letelier, R. M. (2006). Modeling carbohydrate ballasting by
727 *Trichodesmium* spp. *Marine Ecology Progress Series*, 323(Oliver 1994), 35–45.
728 <https://doi.org/10.3354/meps323035>

729 Yang, T., Chen, Y., Zhou, S., & Li, H. (2019). Impact of copper on marine phytoplankton: A Review.
730 *Atmosphere*, 10(414), 599–602. Retrieved from
731 http://inis.iaea.org/search/search.aspx?orig_q=RN:41131251

732 Zehr, J. P., & Capone, D. G. (2020). Changing perspectives in marine nitrogen fixation. *Science*,
733 368(6492). <https://doi.org/10.1126/science.aay9514>

734 Zhang, C., Ito, A., Shi, Z., Aita, M. N., Yao, X., Chu, Q., et al. (2019). Fertilization of the Northwest
735 Pacific Ocean by East Asia Air Pollutants. *Global Biogeochemical Cycles*, 33(6), 690–702.
736 <https://doi.org/10.1029/2018GB006146>

737